ISSN1346－7832

独立行政法人港湾空港技術研究所

# 港湾空港技術研究所報告

# REPORT OF THE PORT AND AIRPORT RESEARCH INSTITUTE

VOL.41 NO.2 June 2002

NAGASE, YOKOSUKA, JAPAN

INDEPENDENT ADMINISTRATIVE INSTITUTION,
PORT AND AIRPORT RESEARCH INSTITUTE

港湾空港技術研究所報告（REPORT OF PARI）
第 41 巻　第 2 号（Vol.41, No.2），2002年6月（June 2002）

# 目　次（CONTENTS）

REPORT OF THE PORT AND
AIRPORT RESEARCH INSTITUTE
Vol.41, No.2 (June 2002)

# Investigation of the Typhoon Pressure and Wind Field with Application for Storm Surge Estimation

**Albena VELTCHEVA***
**Hiroyasu KAWAI****

## Synopsis

The models for estimating storm surge in shallow water regions require as input a realistic atmospheric forcing in the typhoons. In this work, an improvement of the storm surge estimation is proposed by considering the distortion of the pressure distribution and the relevant wind field in land falling typhoons.

The distribution of the pressure and wind in the real typhoon is investigated on the base of data for four typhoons, attacked Kyushu area – T9918, T9119, T9117 and T9307. The validity of Myers radial symmetric pressure distribution is examined. In the front zone of the typhoon, the observed pressure is lower than calculated by Myers formula. The obtained distortion from the radial symmetry of Myers distribution is parameterized as an analytical expression for the modified Myers pressure distribution is proposed. The modified Myers pressure distribution provided closer estimations to the observed ones in comparison with Myers pressure formula.

The influence of the pressure distortion on the wind field in the typhoon is examined. The comparison between observed and calculated wind shows that the previous models underestimated wind, while utilizing modified Myers pressure and taking into account the vertical structure of typhoon by super gradient wind, leads to better agreement with observations.

The response of the storm surge model to the corrected pressure and wind field is checked. Considerations of the pressure distortion and super gradient wind in the typhoon improve the storm surge estimation. More accurate diagnosis of the storm surge magnitude in coastal areas is achieved by the incorporation of the transformation of the typhoon structure due to land approaching and landfalling.

**Key Words**: Distortion of pressure distribution, Typhoon landfall, Super gradient wind, Storm surge, Modified Myers pressure distribution

*Visiting Researcher, Storm Surge and Tsunami Division, Marine Environment and Engineering Department
**Senior Researcher, Marine Environment and Engineering Department
3-1-1 Nagase, Yokosuka 239-0826, Japan,
Phone: +81-468-445052 Fax: +81-468-441274 e-mail: velcheva@ipc.pari.go.jp

港湾空港技術研究所報告
第41巻第2号 (2002.6)

# 高潮推算に用いる台風の気圧と風の場に関する検討

Albena Veltcheva*・河合　弘泰**

要　旨

浅海域において高潮を推算するモデルではその入力条件として現実に近い台風の気圧を与える必要がある．本研究では，上陸した台風の気圧分布のひずみやそれによる風の場を考慮することで高潮の推算方法の改良を試みた．

実際に来襲した台風として，九州地方を襲った台風9918号，9119号，9117号，9307号の4台風をとりあげ，観測データに基づいてこれらの台風の気圧分布や風の場を調べた．Myersによる同心円状の気圧分布は台風の気圧分布を表現するのによく使われているが，この妥当性について確認した．そして，実際に来襲した台風の気圧分布のひずみを表すためのパラメタ化を試み，Myersの気圧分布を修正した気圧分布を表す式を提案した．さらに，この修正した分布による気圧と観測された気圧とを比較した．

次に台風の気圧分布のひずみが風の場に及ぼす影響を調べた．Myersの式で気圧分布を与えると風は過小評価されるが，Myersの気圧分布を修正した気圧分布を用い，さらに超傾度風を考慮することによって，観測風により近い風が得られた．

Myersの気圧分布を修正し，その気圧分布によって風を修正したとき，高潮がどのように変化するかも調べるため，周防灘で観測された高潮と推算した高潮を比較した．沿岸部の高潮を正確に推算するためには，台風が陸地に接近したり上陸したりすることによって台風の構造が変化することを考慮する必要がある．

キーワード：気圧分布のひずみ，台風の上陸，超傾度風，高潮，修正Myers分布

* 海洋・水工部高潮津波研究室
** 海洋・水工部主任研究官
〒239-0826　横須賀市長瀬3-1-1，電話：0468-44-5052，Fax：0468-44-1274，e-mail:velcheva@ipc.pari.go.jp

## CONTENTS

## 1. Introduction

The models for estimating storm surge near the coast require as input a realistic atmospheric forcing in typhoons. The structure of the typhoon changes considerably, when it approaches the land and after landfall due to an increase of the friction of the typhoon air system with the adjacent land surface. The local synoptic and mesoscale factors are essential for accurate reproduction of the actual wind field as Houston et al. (1999) found by investigation of five landfalling typhoons, which generated a significant storm surge.

Several Japanese bays suffer from storm surge disaster phenomenon, generated by typhoons, which attacked Japan. After the worst case of storm surge in Japanese history, produced by the unprecedentedly large typhoon 5915 in 1959 at Ise Bay, different countermeasures were undertaken in order to protect the principal bays of Japan. Unfortunately, in September 1999, typhoon 9918 hit the Kyushu region, generating a large storm surge in the Yatsushiro Sea and the Suo Sea. The detailed description of the damage, caused by T9918, characteristics of the observed storm surge, discussions on the storm surge mechanism and its hindcasting are presented in the special issue of the journal "Umi to Sora" ("Sea and sky") (2001) as well as in Takayama (2001), Kawai et al. (2000) and others. Utilization of the often applied for the case of typhoons Myers pressure distribution for estimating of wind and storm surge, produced significantly smaller values than observed ones for the Suo Sea area. This underestimation can be traced on **Figure 1**, where the data from Kanda Port and the neighbouring Matsuyama, located on the western part of the Suo Sea, are presented. The observed peak value of storm surge is larger from the calculated one by 0.86m, which represents 42 % of the observed value. The estimated wind speed is also strongly undervalued for the case of onshore wind, observed until 7:00 on 24 September 1999. In order to investigate the reasons for these discrepancies and to overcome the observed problems of underestimation of storm surge, the distribution of the pressure and wind in the real typhoon is examined on the base of data for four typhoons, attacked the Kyushu Island in the past – T9918, T9119, T9117 and T9307. Special attention is paid to the western part of the Suo Sea, suffering from high magnitude storm surge during the typhoon 9918.

In this work, an improvement of the storm surge estimation is proposed by considering the distortion of the pressure distribution and the relevant wind field in the landfalling typhoons. The characteristics of the selected four typhoons are briefly presented in **chapter 2**. The atmospheric forcing is described and analyzed in the **chapters 3** and **4**. The validity of Myers radial symmetric pressure distribution is examined. An attempt is made to parameterize the observed distortion in the pressure field of the real typhoon. Analytical expression for the modified Myers pressure distribution is proposed. The comparison between the observed pressure and the calculated one by the modified Myers formula is presented at the end of **chapter 3.**

The influence of the distortion of the pressure distribution on the wind field in the typhoon is studied next in **chapter 4**. Additionally, the vertical structure of a real typhoon is considered as the idea of super gradient wind is applied in the determination of the wind field in the typhoon. A comparison between the estimated magnitude and direction of wind and the measured one is presented at the end of this chapter.

The response of the storm surge model to the corrected pressure and wind field, determined by modified Myers pressure distribution, is examined and the results are shown in **chapter 5**. The modeled storm surge is compared with the measured one at different observation points in the Suo Sea. More accurate diagnosis of the storm surge magnitude in the coastal areas is proposed by the incorporation of the transformation of the typhoon structure due to land approaching and landfalling. At the end, in **chapter 6**, a discussion and concluding remarks are provided.

## 2. Field data

Four typhoons are examined in this work: typhoon No.18 in 1999, denoted as T9918, typhoons No.17 and No.19 in 1991 as T9117 and T9119 and typhoon No.7 in 1993 as T9307. Typhoon 9119 is also known as "apple" typhoon due to the great damage it caused to apple crops in the northern part of Japan. The main characteristics of these four typhoons are listed in **Table 1**.

The detailed description of the characteristics of the typhoon 9918 and its evolution with time is presented in Kawai et al. (2000), Okamura (2001) and Takayama (2001). The routes of the four typhoons considered here are shown on **Figure 2**. All four typhoons affected the Kyushu region, but the route of T9918 was the most landward directed. According to the Japan Meteorological Agency – Okamura (2001), typhoon 9918 passed through Shimo-koshiki Island in Kagoshima Prefecture at around 03:00 (JST) on 24 September and then through the Amakusa Islands. It made a landfall on the northern part of Kumamoto Prefecture at around 06:00. After passing through the northern Kyushu, it made a landfall again on Ube City in Yamaguchi Prefecture before 09:00. Next the typhoon passed through the western Chugoku district and continued to move northeastward with acceleration over the Japan Sea. This land-crossing Kyushu route of T9918 probably affected stronger the typhoon structure in comparison with the other three typhoons considered, whose

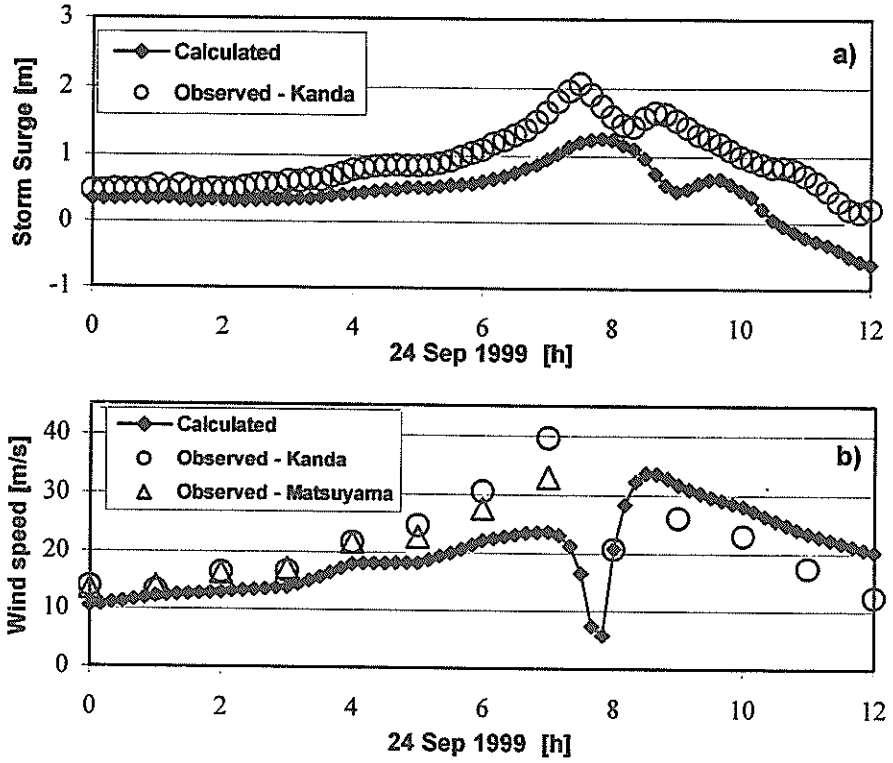


**Figure 1** Comparison between calculated and observed a) storm surge and b) wind speed in the western Suo Sea

**Table 1** Main characteristics of typhoons

| Name of the typhoon | Date | Minimum land registered pressure | Maximum land registered wind speed | Storm surge, registered in the Suo Sea |
|---|---|---|---|---|
| **T9918** | 1999/09/23~09/24 | 943.3hPa<br>24 Sep 03:59<br>Ushibuka | 35.2 m/s SSE<br>22 Sep 21:40<br>Naha | Kanda-207cm<br>24 Sep 07:30<br>Ube-211cm<br>24 Sep 08:00 |
| **T9119** | 1991/09/26~09/28 | 941.1hPa<br>27 Sep 16:26<br>Sasebo | 36.0 m/s S<br>27 Sep 20:10<br>Hiroshima | Aohama-244cm<br>27 Sep 19:00<br>Chofu – 281cm<br>27 Sep 19:00 |
| **T9117** | 1991/09/13~09/14 | 960.6hPa<br>13 Sep 5:46<br>Naha | 37.9 m/s WSW<br>13 Sep 8:00<br>Naha | Aohama –67cm<br>14 Sep 08:00<br>Ube-96cm<br>14 Sep 9:00 |
| **T9307** | 1993/08/09~08/10 | 952.5hPa<br>9 Aug 12:07<br>Naze | 29.1 m/s SE<br>10 Aug 00:10<br>Aburatsu | Aohama-120cm<br>10 Aug 07:00<br>Ube-117cm<br>10 Aug 08:00 |

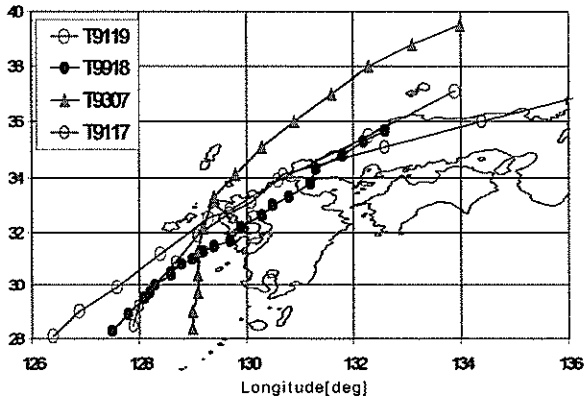


**Figure 2** The routes of typhoons 9918, 9117, 9119 and 9307

are more seaward directed, especially the route of typhoon 9307.

The pressure data, used in this study, were measured every hour at approximately 70 observation points in western Japan. The standard information about the typhoon, latitude and longitude of the typhoon center, radius of maximum winds, central atmospheric pressure and speed of typhoon movement, is utilized for modeling the typhoons, approaching the Kyushu Island.

## 3. Pressure distribution

The primary data requirement for modeling of storm surge is accurate surface wind and atmospheric pressure field. The forcing terms in the storm surge equations are pressure gradient $\nabla p$ and the wind stress $\tau = \rho_a k |\vec{v}| \vec{v}$, where $\rho_a$ is the air density, $k$ is the drag coefficient and $\vec{v}$ is the wind velocity at the anemometer level. Both forcing terms depend on the pressure distribution and therefore the correct determination of pressure reflects on the correct prediction of storm surge.

Widely used for the case of typhoons is Myers formula for pressure, symmetrically distributed with the radial distance $r$ from the center of the typhoon

$$p(r) = p_0 + (p_n - p_0)\exp\left(-\frac{r_0}{r}\right) \qquad (1)$$

Here $r_0$ is the radius of maximum wind and $p_0$ and $p_n$ are the minimum typhoon central pressure and the ambient pressure at a great distance from the eye respectively. The expression (1) is also called negative exponential Schloemer distribution. In the real typhoon however, especially during land approaching and after landfall of typhoon, pressure distribution has not ideal radial symmetry due to influence of the land topography.

### 3.1 Actual pressure distribution in the typhoon and radial symmetry of Myers pressure formula

The distribution of the pressure in the real typhoon is examined on the base of pressure data of four typhoons considered – T9918, T9119, T9307 and T9117. The validity of the Myers radial symmetric pressure distribution is verified on the base of observed pressure. For this purpose, the area surrounding the typhoon center is divided into four sub-areas or zones with respect to the direction of typhoon movement. The scheme of separation is shown on **Figure 3** and sub-areas are named Front, Right, Back and Left zone. The Front zone is defined as the area, enclosed by ±45° from the direction of typhoon movement. Others zones are defined to be a quarter of the area, surrounding typhoon center respectively.

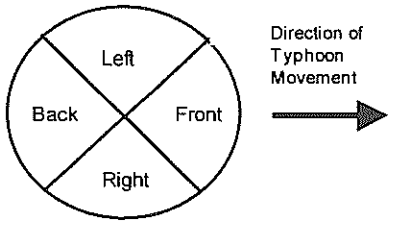


**Figure 3** Scheme of the separation of the typhoon area into 4 zones

The observed pressure distribution is compared with Myers distribution, determined by equation (1). The difference between observed and calculated by (1) pressure is determined

$$\Delta p_i = p_i^{obs} - p_i^{Myers} \quad for \quad i = 1, N \qquad (2)$$

where $p_i^{obs}$ and $p_i^{Myers}$ are respectively observed and calculated by (1) pressure for the observation point $i$ and $N$ is the number of observation points.

For each sub-area the difference $\Delta p_i$ is averaged over the all points, which are located in the corresponding area for the given observation term. For the Front area, for example, the averaged difference is

$$\Delta p^{Front} = \frac{\sum_{i}^{N_{Front}} \Delta p_i}{N_{Front}} \qquad (3)$$

and $N_{Front}$ is a total number of the points, located in the Front zone for given term of observation. In the same way the $\Delta p^{Right}$, $\Delta p^{Back}$ and $\Delta p^{Left}$ are determined.

The comparison between Myers formula (1) and the observed pressure distribution was performed for the cases, when the typhoons passed close to the Kyushu area. For T9918 the data of 24 September 1999 from

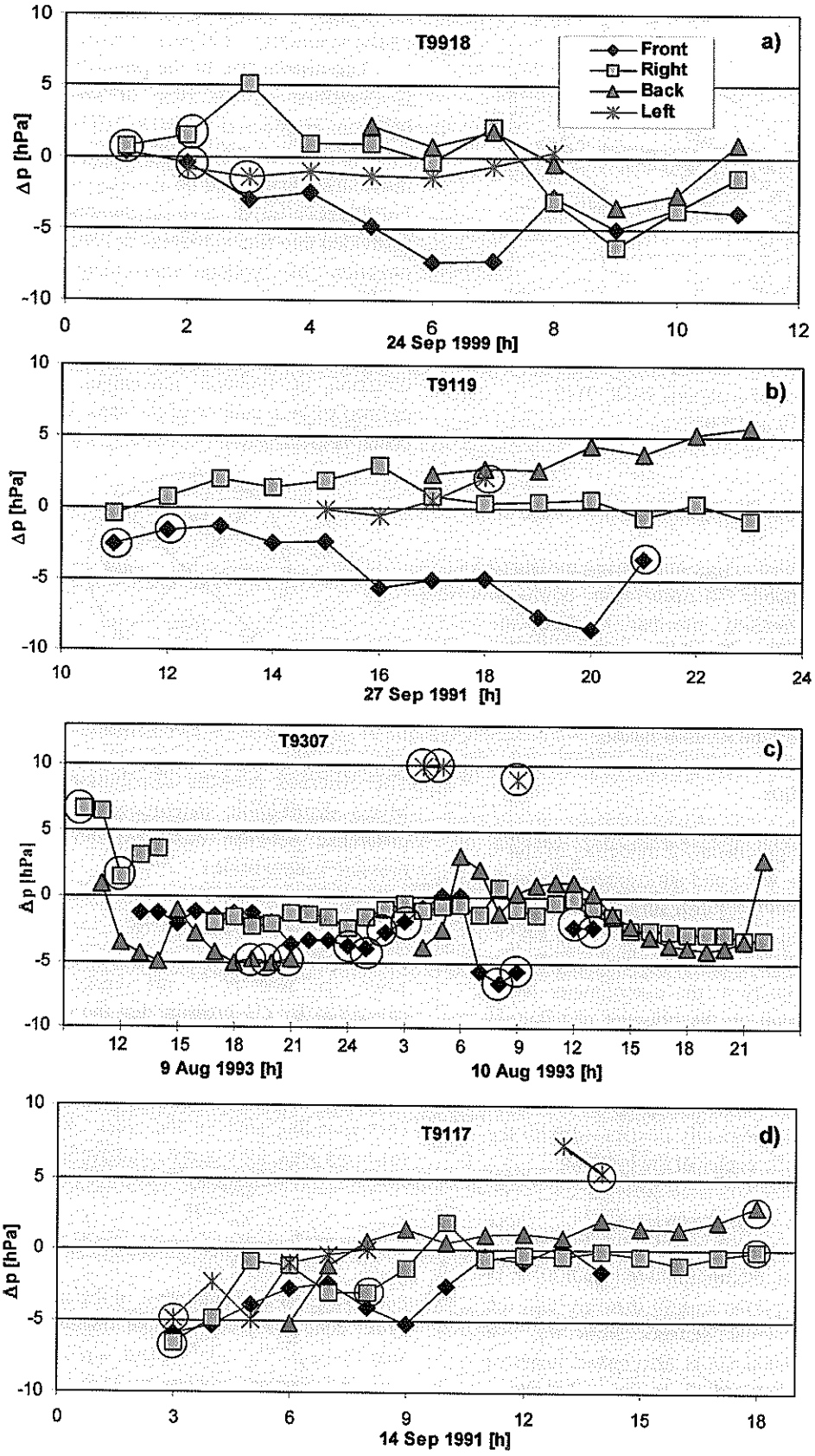


**Figure 4** The variation of $\Delta p$ with time for typhoon a)9918; b)9119; c)9307 and d)9117

01:00 until 11:00 are considered, for T9119 - the data of 27 September 1991 from 11:00 to 23:00, for T9307 - from 11:00 on 9 August 1993 until 22:00 on 10 August 1993 and for T9117 - the data of 14 September 1991 from 03:00 to 18:00.

The variation of averaged for each zone pressure difference $\Delta p$ during the observations terms can be traced on **Figure 4 (a), (b), (c)** and **(d)** for T9918, T9119, T9307 and T9117 respectively.

In this comparison only the observation points with a distance to the typhoon center less than three times radius of maximum wind $r_0$ ($r < 3r_0$) are considered, in order to exclude the influence of the other baric formations. On **Figure 4** the circled points are data, estimated by only one observation. They are classified as less reliable data from a statistical point of view and are excluded from further consideration. The analysis of pressure field needs information about observed pressure in each of the four considered typhoon zones, schematically presented on **Figure 3**. Unfortunately, due to peculiarities of the typhoon route, especially for the most seaward oriented T9307, this requirement cannot be satisfied for each of observation terms considered. In order to ensure statistical reliable results, only observation terms with available data from at least three typhoon zones are chosen in further investigation.

The main peculiarity, which can be easily traced for the typhoons T9918 and T9119 is, that in the Front zone of the typhoon the observed pressure is always less than the calculated by Myers formula (1). The same tendency, although not so well pronounced, is observed also for the remaining two typhoons T9307 and T9117.

### 3.2 Modified Myers pressure distribution

The results of investigation of pressure fields in the real typhoons provoke an idea to modify Myers formula (1) for pressure distribution. In order to incorporate the observed distortion of the pressure field of real typhoon, a new analytical expression for pressure distribution is proposed in the form

$$p(r,\theta) = p_0 + (p_n - p_0)\exp\left[-\frac{r_0(\theta)}{r}\right] \qquad (4)$$

The essential difference in this expression from Myers formula (1) is the dependence of pressure on the angle $\theta$ between observation point and the direction of typhoon movement, additionally to dependence on the distance to the typhoon center by $r$. This dependence on the angle $\theta$ is included through the radius of maximum wind $r_0$ in the form

$$r_0(\theta) = \overline{r}_0 + r_{01}\cos(\theta - \alpha_1) + r_{02}\cos(2\theta - \alpha_2) \qquad (5)$$

Thus the radius of maximum wind $r_0$ here is a function of angle $\theta$ in contrast of constant radius in the Myers formula (1). The five parameters $(\overline{r}_0, r_{01}, r_{02}, \alpha_1, \alpha_2)$, which appeared additionally in (5), are proposed to be estimated by the least squares method on the base of observed pressure data.

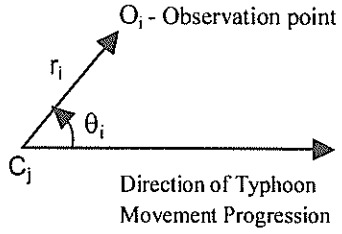


**Figure** 5 Scheme of location of observation point with respect to typhoon

Using the coordinates of the typhoon position, at each observation term $j$ the distance $r_i$ from the center of the typhoon $C_j$ to the observation point $O_i$ and the angle $\theta_i$ between the direction of typhoon movement and the observation point $O_i$ is determined as shown on **Figure 5.** Therefore, each observation point $O_i$ at each observation term $j$ is characterized by triple $(r_i, \theta_i, p_i^{obs})$, where $p_i^{obs}$ is the measured pressure in the observation point $O_i$ for the given $j$ observation term.

The functional of differences $a^2$ is created

$$a^2 = \sum_{i=1}^{n}\left[p(r_i,\theta_i;\overline{r},r_{01},r_{02},\alpha_1,\alpha_2) - p_i^{obs}\right]^2 \qquad (6)$$

where $p(r_i,\theta_i;\overline{r},r_{01},r_{02},\alpha_1,\alpha_2) = p_c + (p_n - p_c) *$

$$* \exp\left[-\frac{\overline{r}_0 + r_{01}\cos(\theta_i - \alpha_1) + r_{02}\cos(2\theta_i - \alpha_2)}{r_i}\right]$$

and then $a^2$ is minimized in order to determine the five parameters in the modified Myers distribution as a solution of the system

$$\frac{\partial a^2}{\partial \overline{r}_0} = 0, \quad \frac{\partial a^2}{\partial r_{01}} = 0, \quad \frac{\partial a^2}{\partial r_{02}} = 0, \quad \frac{\partial a^2}{\partial \alpha_1} = 0, \quad \frac{\partial a^2}{\partial \alpha_2} = 0 \qquad (7)$$

for each observation term $j$.

The parameters $(\overline{r}_0, r_{01}, r_{02}, \alpha_1, \alpha_2)$ of the modified Myers pressure distribution (4) are listed in the **Table 2 (a), (b), (c)** and **(d)** for T9918, T9119, T9117 and T9307 respectively.

**Table 2** Parameters of modified Myers pressure distribution

**(a)** T9918

| 24-Sep-99 | $\overline{r}_0$ | $r_{01}$ | $r_{02}$ | $\alpha_1$ | $\alpha_2$ |
|---|---|---|---|---|---|
| [h] | [km] | [km] | [km] | [rad] | [rad] |
| 5 | 56.0 | 9.69 | -2.93 | 0.05 | -3.03 |
| 6 | 59.5 | 10.80 | -7.06 | -0.13 | 2.70 |
| 7 | 57.6 | 13.50 | -3.21 | -0.16 | 1.80 |
| 8 | 52.5 | 5.75 | -3.52 | -1.24 | 0.94 |
| 9 | 80.4 | 21.76 | -9.91 | -0.21 | -1.67 |
| 10 | 72.1 | 16.70 | -12.59 | -0.68 | -2.49 |
| 11 | 102.8 | 41.92 | -21.98 | 1.38 | 0.25 |

**(b)** T9119

| 27-Sep-91 | $\overline{r}_0$ | $r_{01}$ | $r_{02}$ | $\alpha_1$ | $\alpha_2$ |
|---|---|---|---|---|---|
| [h] | [km] | [km] | [km] | [rad] | [rad] |
| 15 | 80.9 | 0.46 | 9.29 | 0.90 | 0.14 |
| 16 | 82.8 | 14.89 | 11.17 | -0.02 | -0.21 |
| 17 | 89.4 | 18.26 | 6.45 | 0.10 | -0.28 |
| 18 | 94.4 | 21.38 | 3.81 | 0.09 | 0.19 |
| 19 | 108.1 | 39.66 | -10.64 | 0.48 | -2.23 |
| 20 | 101.4 | 35.67 | -5.50 | 0.22 | -2.69 |
| 21 | 91.5 | 7.61 | -12.16 | -0.14 | 1.22 |

**(c)** T9117

| 14-Sep-91 | $\overline{r}_0$ | $r_{01}$ | $r_{02}$ | $\alpha_1$ | $\alpha_2$ |
|---|---|---|---|---|---|
| [h] | [km] | [km] | [km] | [rad] | [rad] |
| 3 | 54.4 | 1.49 | -4.89 | 0.88 | 1.31 |
| 4 | 48.1 | 11.66 | -0.35 | -0.41 | -3.07 |
| 5 | 56.0 | -3.08 | 9.01 | -0.90 | -0.88 |
| 6 | 57.0 | -10.29 | 16.43 | -0.20 | -1.02 |
| 7 | 57.4 | 7.19 | 7.97 | -1.23 | -1.54 |
| 8 | 62.5 | 16.23 | -9.62 | -1.22 | 0.64 |
| 9 | 70.6 | 25.26 | 3.19 | -0.08 | 2.03 |
| 11 | 71.7 | 13.16 | 2.75 | -0.07 | 0.31 |

**(d)** T9307

| 10-Aug-93 | $\overline{r}_0$ | $r_{01}$ | $r_{02}$ | $\alpha_1$ | $\alpha_2$ |
|---|---|---|---|---|---|
| [h] | [km] | [km] | [km] | [rad] | [rad] |
| 4 | 95.6 | 3.93 | 11.71 | -2.44 | -0.80 |
| 5 | 83.0 | -19.41 | 5.02 | 1.74 | 2.52 |
| 6 | 95.3 | -1.97 | -13.22 | 2.12 | 0.17 |
| 7 | 124.9 | 26.91 | 5.50 | 0.74 | 1.98 |
| 8 | 107.4 | 4.06 | -9.06 | -0.34 | 1.68 |
| 9 | 101.7 | 26.85 | -15.89 | -0.95 | 2.92 |

Here only the terms, when the data of at least 3 zones, surrounding the typhoon center were available, are considered in the determination of the parameters of the modified Myers pressure distribution (4). These parameters are used next for modeling the pressure and wind field in the typhoon.

The variation of the radius of the modified Myers pressure distribution with time for T9918 and T9119 is

shown on **Figure 6**. The evolution of modified Myers pressure distribution for T9918 from 5:00 to 10:00 on 24 September, 1999 is presented on **Figure 7**. The origin of coordinate system is located at the center of the typhoon, while the positive part of the x-axis is the direction of the typhoon movement progression. There is a well-pronounced distortion of the radius of maximum wind $r_0(\theta)$ and respectively of pressure distribution from the radial symmetry of Myers formula (1).

### 3.3 Comparison between observed and calculated pressure

The accuracy of the new proposed formula for pressure distribution (4) and Myers formula (1) is checked. The comparison between observed $p_i^{obs}$ and calculated pressure for one observation term 6:00 on 24 September, 1999 is shown on **Figure 8**. The digits, placed close to the data, noted the location of the observation point in the different zones, according to the separation made on **Figure 2**, as 1 is for the Front zone, 2 is for the Left zone, etc. In most cases, the modified Myers pressure, calculated by (4), provided closer estimation to the observed pressure in comparison with the Myers formula (1).

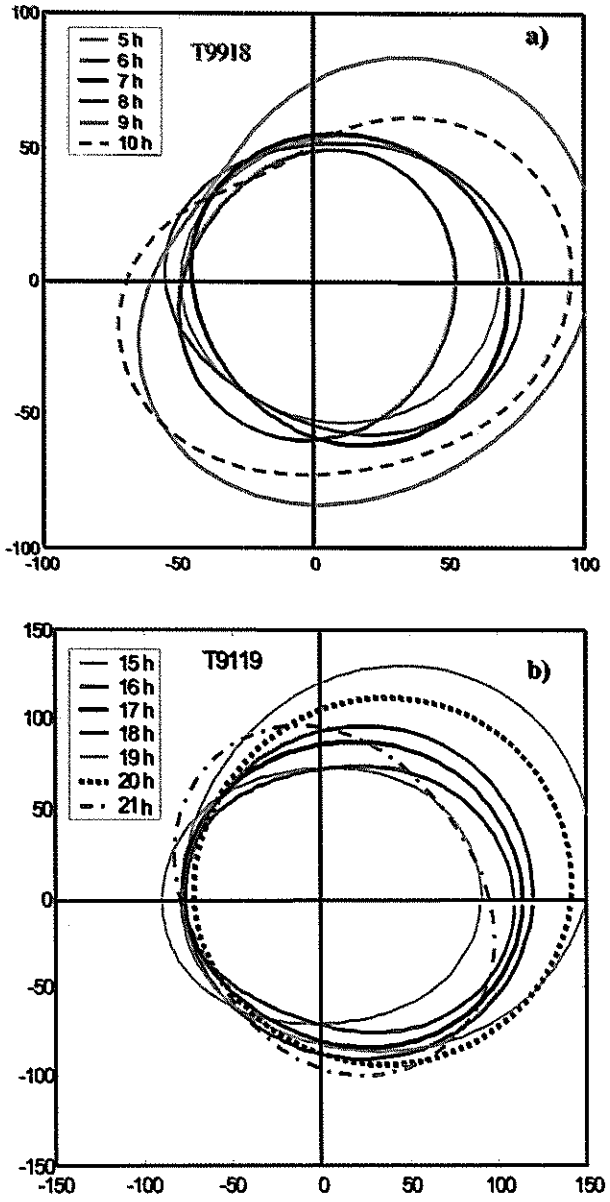


**Figure 6** Variation of the radius $r_0(\theta)$ of the modified Myers distribution with time for a) T9918 and b) T9119

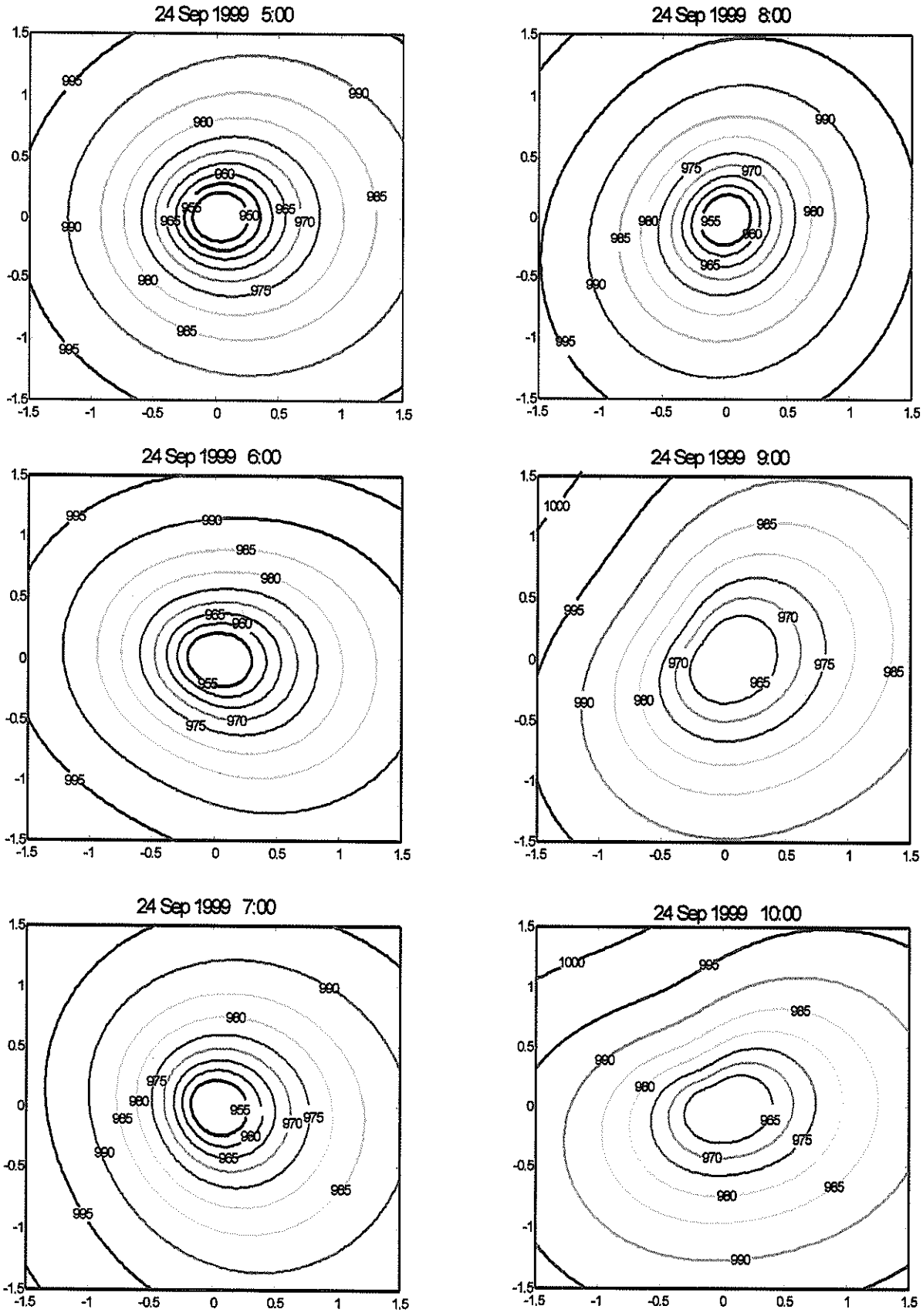


**Figure** 7 Time evolution of modified pressure distribution of T9918

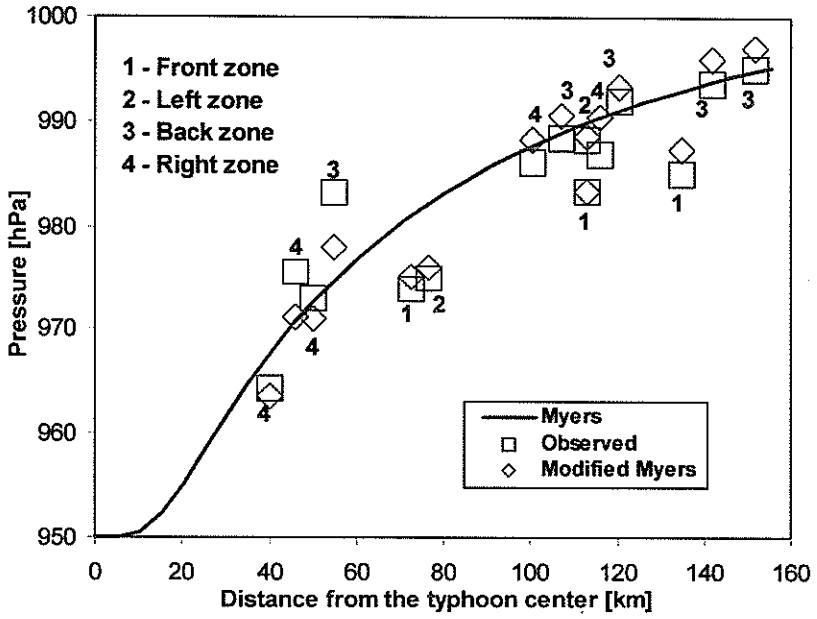


**Figure 8** Comparison between estimated and observed pressure

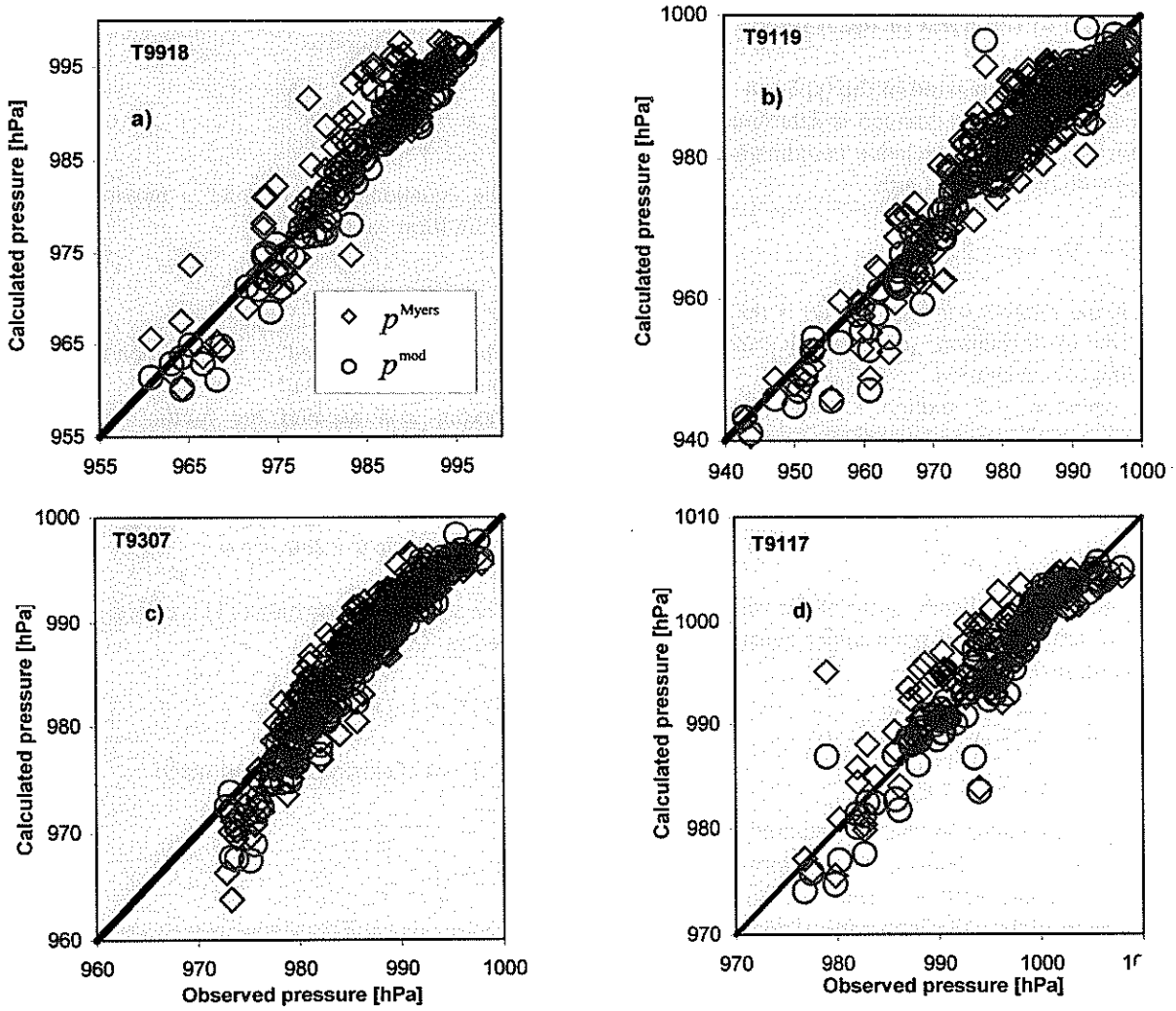


**Figure 9** Comparison between observed $p^{obs}$ and calculated by Myers $p^{Myers}$ and by modified Myers pressure $p^{mod}$ for a)T9918; b) T9119; c)T9307 and d) T9117

The calculated pressure by Myers $p^{Myers}$ (diamonds) and by modified Myers $p^{mod}$ (open circles) pressure distribution is compared with observed ones on **Figure 9,** as all pressure data are used. This analysis is performed for each of the considered four typhoons. The overestimation of the pressure by Myers formula is most pronounced for the case of T9918 on **Figure 9 (a),** whose structure is affected strongest by the presence of land in comparison with the other typhoons, considered in this study. Consequently, underestimation of the magnitude of the storm surge due to this overestimated pressure field, can be expected.

On the base of the above analysis it can be concluded that the modified Myers pressure distribution, estimated by (4), provided better approximation of the observed pressure distribution in the real typhoon in comparison with the radial symmetrical Myers distribution.

## 4. Distribution of the wind in the typhoon

### 4.1 Determination of the wind in the typhoon

The wind speed in the typhoon is determined from the equation of motion in a relative coordinate system, firmly fixed with the rotating Earth

$$\frac{d\vec{v}}{dt} = \frac{1}{\rho_a}\nabla p - \vec{\gamma}_e - 2\vec{\omega}\times\vec{v} \tag{8}$$

where $\vec{v}$ is the relative wind speed, $\vec{\omega}$ is the angular velocity of the earth rotation, $\rho_a$ is the air density, $\vec{\gamma}_e$ is the centrifugal acceleration.

This equation of motion, written in polar coordinates for stationary and steady tangential motion, is reduced to

$$\frac{v_\theta^2}{r} + 2\omega v_\theta \sin\varphi = \frac{1}{\rho_a}\frac{\partial p}{\partial r} \tag{9}$$

Here $v_\theta$ is the tangential component of the velocity $\vec{v}$ and $\varphi$ is the latitude in the point under consideration. The solution of this equation

$$v_\theta = -\frac{fr}{2} + \sqrt{\left(\frac{fr}{2}\right)^2 + \frac{r}{\rho_a}\frac{\partial p}{\partial r}} \tag{10}$$

is called a gradient wind as the substitution with the Coriolis parameter $f = 2\omega\sin\varphi$ is performed. The magnitude of gradient wind is given by (10) and the direction is tangential to the trajectory of motion. The assumption is made that isolines of pressure and trajectory of motion do not cross each other. Therefore, the direction of gradient wind is also tangential to the pressure isolines.

The progressive movement of the typhoon air system is additionally taken into account by

$$\frac{d\vec{v}}{dt} = \frac{1}{\rho_a}\nabla.p - \vec{\gamma}_e - 2\vec{\omega}\times\left(\vec{v}+\vec{C}\right) \tag{11}$$

where $\vec{C}$ is the speed of typhoon movement.

The equation (11) is similar to equation (8), as the difference is that the Coriolis force is now acting on the vector sum $\left(\vec{v}+\vec{C}\right)$. Therefore, equation (9) for the tangential component of the wind speed is transformed into

$$\frac{v_\theta^2}{r} + 2\omega v_\theta \sin\varphi + 2\omega C\sin\theta\sin\varphi = \frac{1}{\rho_a}\frac{\partial p}{\partial r} \tag{12}$$

where $\theta$ is the angle between the observation point and direction of typhoon movement. This equation is also called the cyclonic gradient flow equation for moving typhoon in Murty (1984) and Gonnert et al. (2001). Another form of this equation is given by Fujii and Mitsuta (1986), introducing the inertial radius $r_i$ for a moving typhoon as

$$\frac{1}{r_i} = \frac{1}{r}\left(1 + \frac{C}{v_\theta}\sin\theta\right) \tag{13}$$

and the equation of motion for a moving typhoon is written in form, similar to (9)

$$\frac{v_\theta^2}{r_i} + 2\omega v_\theta \sin\varphi = \frac{1}{\rho_a}\frac{\partial p}{\partial r} \tag{14}$$

The wind, calculated by the equation (14), is called friction-free wind (FFW).

Taking into account the inertial radius for the moving typhoon, the equation (12) can be written also in the form

$$\frac{v_\theta^2}{r} + \frac{v_\theta C}{r}\sin\theta + 2\omega v_\theta \sin\varphi = \frac{1}{\rho_a}\frac{\partial p}{\partial r} \tag{15}$$

The solution of equation (15) is called gradient wind, denoted as $U_G$

$$U_G = V_c\left(\sqrt{\gamma^2+1} - \gamma\right) \tag{16}$$

where $V_c$ is cyclostrophic wind speed

$$V_c = \sqrt{\frac{r}{\rho}\frac{\partial p}{\partial r}} \tag{17}$$

and parameter $\gamma$ is given by

$$\gamma = \frac{1}{2}\left(\frac{C\sin\theta}{V_c} + \frac{V_c}{V_g}\right) \tag{18}$$

The wind, distant from the center of typhoon, is determined as

$$V_g = \frac{1}{2\rho_a \omega \sin\varphi} \frac{\partial p}{\partial r} \tag{19}$$

and is called geostrophic wind .

**4.2 Super gradient wind in the typhoon**

The air motions in the typhoon are considered plane, neglecting completely the vertical structure of typhoon, in the above consideration of the wind. In the reality, on the other hand, there are considerable vertical motions in the typhoon, which lead to changes in the wind distribution - Shea and Gray (1973) and Gray and Shea (1973). Generally, the wind vector crosses isobars. The angle, made by wind vector with the isobars is denoted as the *inflow angle* – Gray and Shea (1973), as the *angle of deflection* - by Pagenkof and Pearce (1975) and Mitsuta et al. (1980) and as the *ingress angle* by Jelesnianski (1965). Considering the inflow angle $\alpha$, the wind speed in the typhoon has to be determined as

$$V = U_G \cos\alpha \tag{20}$$

Gray and Shea (1973), using the flight data of the National Hurricane Research Laboratory, solved numerically the equation, required for the super-gradient wind and determined the inflow angle. Their conclusion is that the inflow angle is small for radial distance, less than radius of maximum wind $r_0$, became 10° for $r_0$ and increases to 25° for twice $r_0$, but $\alpha$ increases unrealisticically for larger radii.

Myers and Malkin (1961) determine the angle of inflow for stationary storm, which varies from $\alpha = 0°$ at the center to $\alpha \approx 30°$ at radial distance three times the radius of maximum wind and constant after that.

For the Probable Maximum Hurricane (PMH), Murty (1984) reported that the angle of inflection is

$$\begin{aligned} 0 < \alpha < 10° \quad & for \quad r < r_0 \\ 10° < \alpha < 25° \quad & for \quad r_0 < r < 1.2r_0 \\ \alpha = 25° \quad & for \quad r > 1.2r_0 \end{aligned} \tag{21}$$

where $r_0$ is again the radius of maximum wind.

The inflow angle $\alpha$ in different observation stations around Japan was statistically investigated by Mitsuta et al. (1980). The inflow angle varies remarkably with the direction of friction free wind and from station to station.

The radial wind field is constructed by rotating the flow to a constant inflow angle. As first approximation in the present work, the inflow angle $\alpha$ is proposed to be 30° and no dependence on typhoon radius is supposed.

The model of Fujii and Mitsuta (1986) is utilized here for the determination of magnitude of super gradient wind by

$$V_{super} = C_1(x) U_G \tag{22}$$

The coefficient $C_1(x)$ is a function of the distance from the typhoon center

$$C_1(x) = C_1(\infty) + \left[C_1(x_p) - C_1(\infty)\right]\left(\frac{x}{x_p}\right)^{k-1} * \\ * \exp\left\{\left(1 - \frac{1}{k}\right)\left[1 - \left(\frac{x}{x_p}\right)^k\right]\right\} \tag{23}$$

where $x = r/r_0$, $x_p = 0.5$, $k = 2.5$, $C_1(\infty) = 0.6667$ and $C_1(x_p) = 1.2$. In the previous models the coefficient $C_1(x)$ is fixed to a constant value 0.6 or 0.7. The above formula (23) also gives in first approximation $C_1(x) = C_1(\infty) = 0.6667$.

**4.3 The effect of pressure distortion and super gradient wind on the estimated wind**

The obtained distortion of pressure distribution in the real typhoon affects the wind field. The coefficient $C_1(x)$, calculated by constant radius of maximum wind $r_0$ of Myers pressure distribution (1), differs from that calculated by variable radius $r_0(\theta)$ of modified Myers pressure (4). The variation of the coefficient $C_1(x)$ in the four typhoon zones is presented on **Figure 10** for both, Myers and modified Myers pressure distribution. For the observation term 7:00 on 24 September, 1999, the distortion of the radius of maximum wind results into shifting the coefficient $C_1(x)$ for modified Myers, presented by blue line with respect to $C_1(x)$ for Myers pressure – red line. In the Front zone for $0.7 \le x \le 1.5$, the coefficient $C_1(x)$ for modified Myers pressure distribution is higher than $C_1(x)$ for Myers and this leads to expansion of the area with strong wind. In the Back zone the opposite tendency is observed. No significant difference is found in the Left and in the Right zone and two curves almost overlapped each other in these zones.

The wind field in the typhoon is estimated by using Myers (1) and modified Myers (4) pressure distribution as the super gradient wind is calculated by (22). On **Figure 11** the estimated wind distribution for

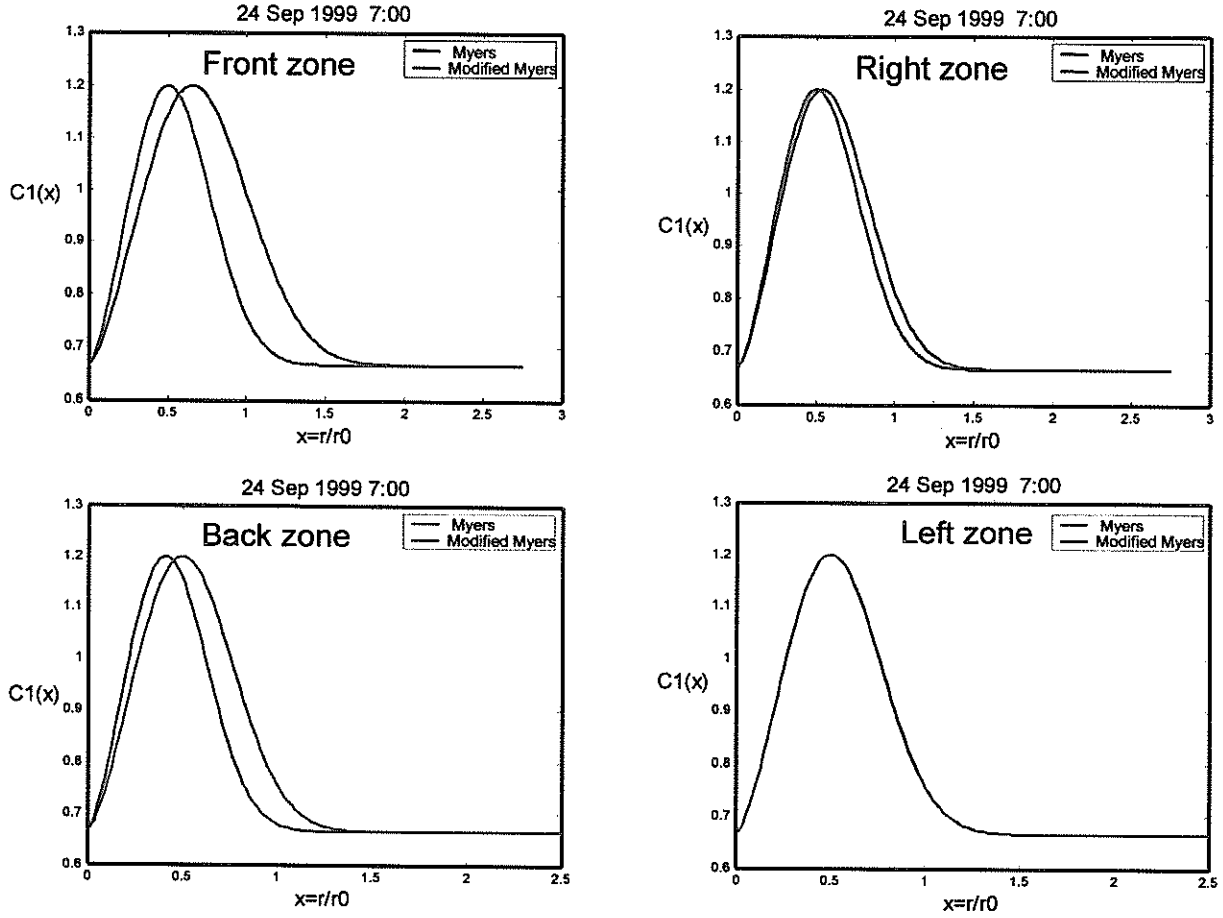


**Figure 10** Coefficient $C_1(x)$ in different zones of typhoon

the observation term 7:00 on 24 September, 1999 is shown. The origin of the coordinate system is located in the center of the typhoon for each observation term and the positive part of the x-axis is the direction of typhoon movement.

The wind, calculated by Myers pressure formula without considering super gradient wind $\vec{V}^{Myers}$ is shown on **Figure 11 (a)**, while on **Figure 11 (b)** the super gradient wind is additionally taken into account in the determination of $\vec{V}^{Myers}_{super}$. The wind, estimated by the modified Myers pressure distribution and including the effect of super gradient wind - $\vec{V}^{mod}_{super}$ is shown on **Figure 11 (c)**.

The influence of the pressure distortion and the super gradient wind on the wind distribution in the typhoon is then studied and the results are presented on **Figure 11 (d), (e)** and **(f)**. The open circles are the positions of observation points, where pressure data are measured. The effect of only super gradient wind can be seen on **Figure 11 (d)**, where the difference $\left|\vec{V}^{Myers}_{super}\right| - \left|\vec{V}^{Myers}\right|$ between wind field of **Figure 11 (b)** and **Figure 11 (a)** are shown. The warm colors mean positive difference, while cold colors denote a negative one. The inclusion of super gradient wind gives higher values of estimated wind in the area close to the radius of maximum wind.

The effect of the pressure distortion is examined on **Figure 11 (e)** by the difference $\left|\vec{V}^{mod}_{super}\right| - \left|\vec{V}^{Myers}_{super}\right|$ between the wind of **Figure 11 (c)** and **Figure 11 (b)**. In the front zone of the typhoon, the wind, calculated by modified Myers pressure is higher than calculated by Myers. On the **Figure 11 (f)**, the combined effect of distortion of pressure distribution and super gradient wind is examined by difference $\left|\vec{V}^{mod}_{super}\right| - \left|\vec{V}^{Myers}\right|$ of wind field of **Figure 11 (c)** and **Figure 11(a)**. The combination of distorted pressure distribution through the modified Myers pressure distribution and the super gradient wind, calculated by the variable coefficient $C_1(x)$, leads to increasing the wind speed in the area, close to the radius of maximum wind of the typhoon in comparison with Myers pressure and constant coefficient $C_1$.

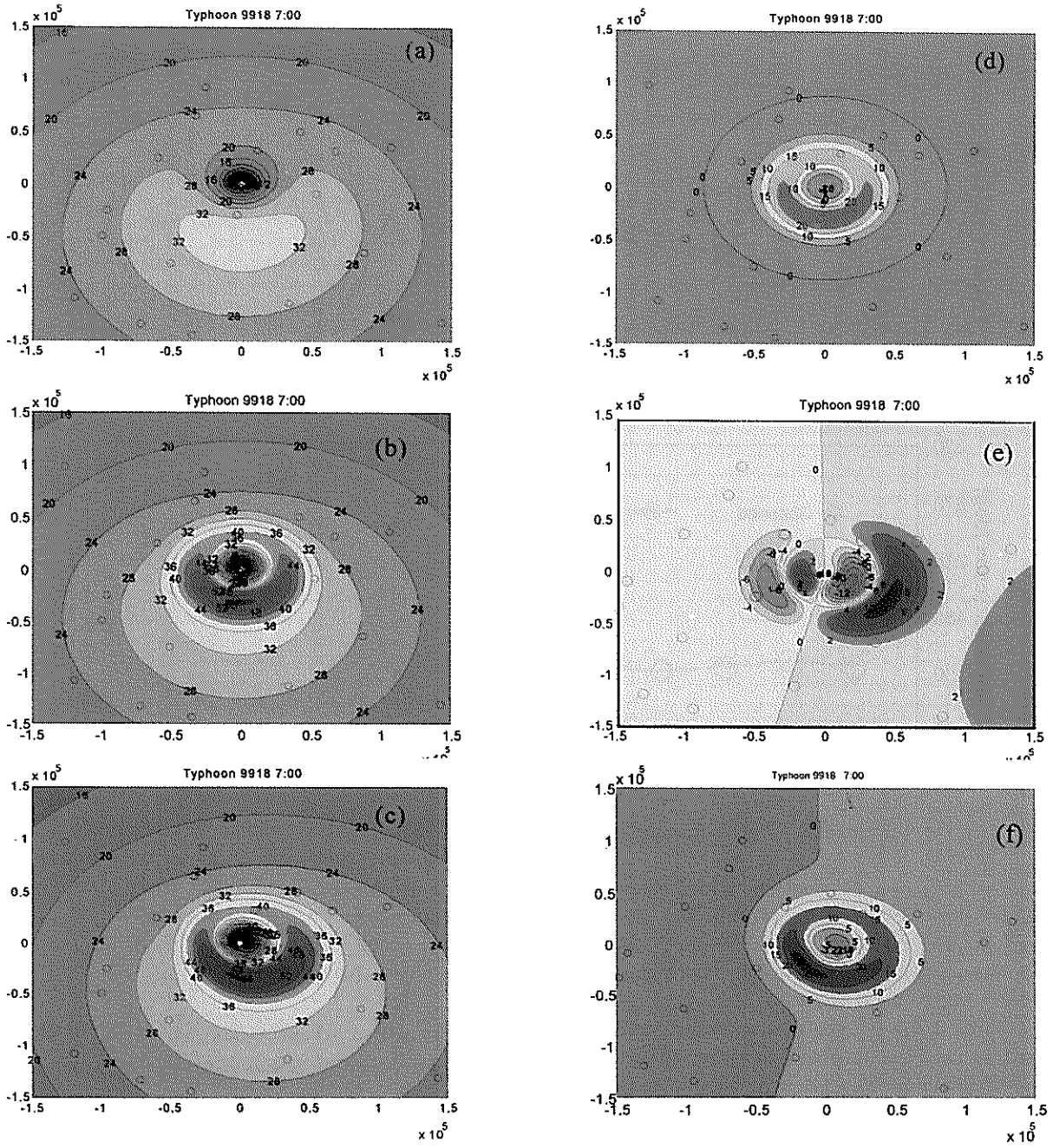


**Figure 11** Estimated wind a) by Myers pressure distribution; b) by Myers pressure distribution and super gradient wind; c) by modified Myers pressure distribution and super gradient wind;
Investigation of d) effect of super gradient wind; e) effect of pressure distortion; f) combine effect of d) and e).

### 4.4 Comparison between observed and calculated wind

The wind data, measured at land located stations, are usually largely affected by the local topographical conditions and the comparison with calculated wind became difficult. Thus, not all wind data from the observation stations, used in this study, can be considered as representative for the comparison with the modeled wind. In principle, the wind speeds over land are much less than those over water. For the storm surge modeling the wind over water, also called marine wind, is important. In the present work, the wind data are land measured and ones over water are missing.

The transition of the typhoon boundary layer wind from open sea to landfall is investigated by Power (1982). A rich database was used for this purpose, including flight data over water. It was found that the overland wind is approximately 80% of that of over water wind, measured offshore.

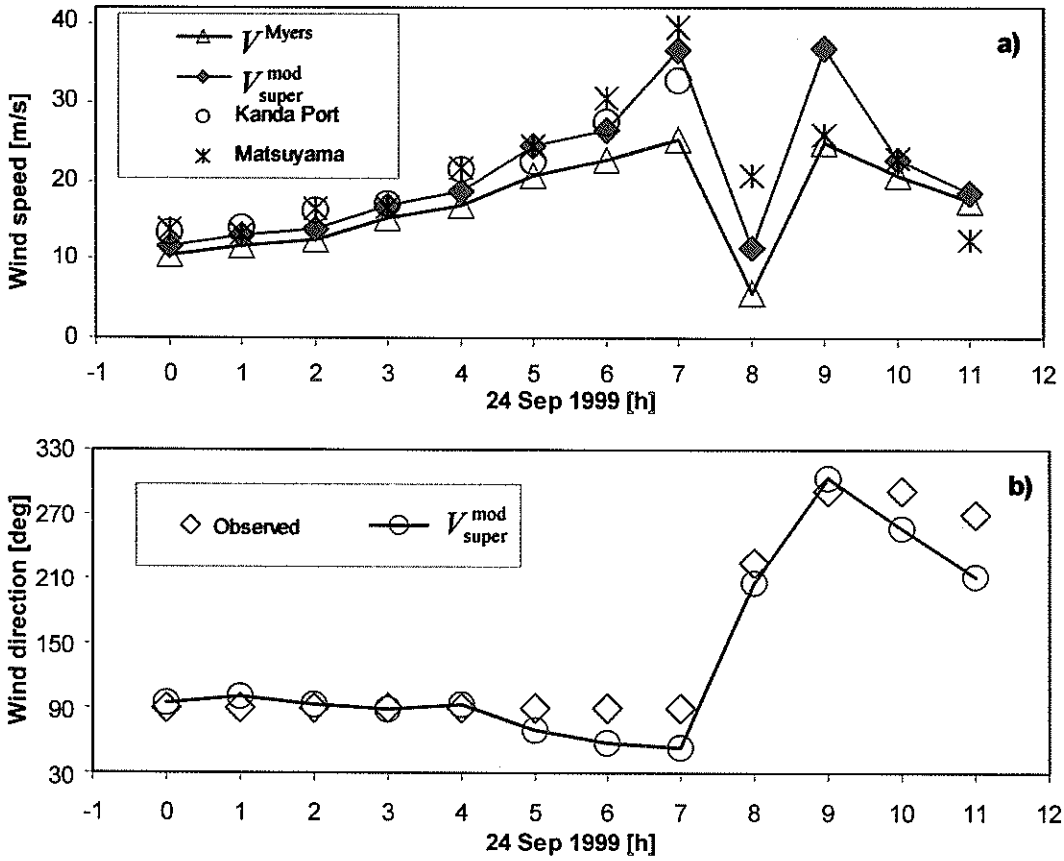


**Figure 12** Magnitude and direction of calculated and observed wind in the western Suo Sea

The time variation of wind speed and direction, measured in the western part of the Suo Sea, is compared with the calculated one on **Figure 12**. The observed data were recorded at Kanda Port and at the neighbouring Matsuyama. The wind at Kanda Port was measured about 2 km off the port and these data are considered as the most reliable and representative for the marine wind in the Suo Sea. The magnitude of the observed wind at Kanda Port and Matsuyama is shown by open circles and stars respectively. The wind, calculated by previous models - $V^{Myers}$, presented by triangles on **Figure 12 (a)**, is smaller than the observed wind speed. Utilization of the modified Myers pressure and additionally considering super gradient wind in the determination of $V^{mod}_{super}$, provided closer estimation to the observed wind speed on the **Figure 12 (a)**. The calculated wind directions for $V^{mod}_{super}$, shown by circles on **Figure 12 (b)**, also agree well with measured ones for this observation station. In this figure the north direction is determined by 0 degree, east – by 90 degree, south is 180 degree and west is 270 degree respectively.

The data only from coastal located observation stations and additionally only with onshore directed wind are compared with estimated ones on **Figure 13**. Again if Myers pressure is used, the wind is underestimated, while consideration of pressure distortion and super gradient wind leads to better agreement with observations.

## 5. The effect of pressure distortion and super gradient wind on the magnitude of storm surge

The results of the investigation of the pressure and wind field in the real typhoon, presented and discussed at the previous chapters, are applied next for the determination of the of storm surge. The response of the storm surge model to the distorted pressure field and super gradient wind is examined.

The storm surge model, used in this study, is a 2-D depth averaged numerical model with multiple grids. A coarse grid is applied for the offshore region and three different meshes with grid size 16.2 km, 5.4 km and 1.8 km respectively are used. In the shallow coastal area, finer grids are utilized as their grid size varies from 0.2 km to 0.6 km. The peculiarities of the storm surge model are discussed in details by

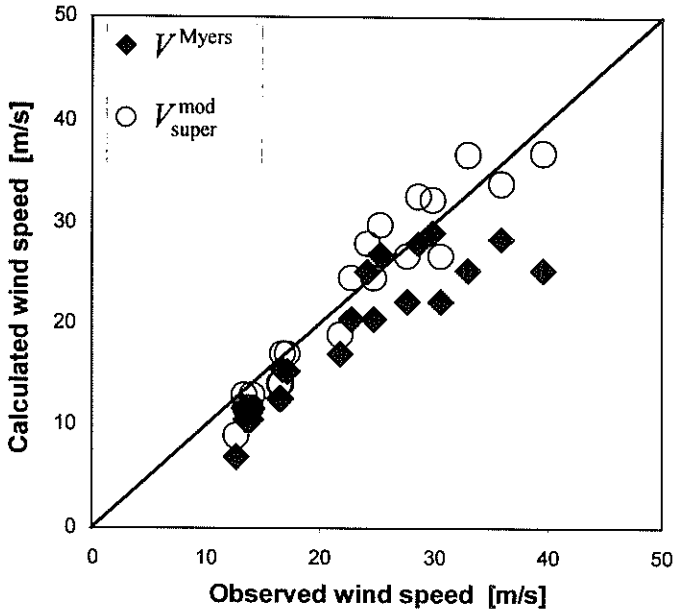


**Figure 13** Comparison between calculated and observed wind in the Suo Sea

Kawai et al. (2000).

The time variation of the magnitude of storm surge, estimated and recorded at Kanda Port, in the western part of the Suo Sea, is shown on **Figure 14.** Significant improvement of storm surge estimation is achieved by consideration of pressure distortion and super gradient wind in contrast with previous models, presented by diamonds on **Figure 14.** The peak of the new estimated storm surge $\eta^{mod}_{super}$ is slightly higher than the observed by 0.17m, which is 8.2% of the observed value. The variation of storm surge, before the peak, is estimated accurately. However, after the peak of the storm surge, the typhoon center was located to the north of the Suo Sea and the direction of the wind was from land to sea. The model overestimates the wind speed after the changes of the wind direction, as can be traced on **Figure 12 (a).** That is the reason for the dropping of the estimated storm surge so rapidly. Additional research is needed in order to overcome this problem.

The maximal magnitude of the storm surge, recorded in different observation points in the Suo Sea is compared with the calculated one on **Figure 15.** The thin line presents the storm surge $\eta^{Myers}$, determined by the previous model, while thick line is estimated storm surge $\eta^{mod}_{super}$, estimated considering modified Myers pressure and super gradient wind. The observed data has a different rank of reliability, as "A" denotes the highest reliability and "D" is lowest. The "A" data are from tide records, while "B" to "D" data are inundation traces or witness by affected persons. The detail description of these field data and the criteria for their classification are presented by Kawai et al. (2000).

The observed improvement of storm surge estimation in the Suo Sea area, presented on **Figure 15,** is quantitatively expressed by checking the ratio between the calculated and observed magnitude of storm surge. The ratio $\eta^{Myers}/\eta_{obs}$ of the calculated storm surge by previous model to the observed one is shown by diamonds on **Figure 16,** while the circles are the ratio $\eta^{mod}_{super}/\eta_{obs}$ of storm surge, estimated by considering the distortion of pressure distribution and super gradient wind to the observed one. It is well-seen tendency of underestimation of storm surge by the previous model, especially in the western Suo Sea. The mean value of the ratio $\eta^{Myers}/\eta_{obs}$ is 0.74. Except for the eastern part of the Suo sea – Shin-nan-yo and Tokuyama observation points, the utilizing the modified Myers pressure and super gradient wind as input in the storm surge model improves the storm surge estimation as in average the ratio $\eta^{mod}_{super}/\eta_{observed}$ is 1.03. The observed discrepancy for the above mentioned two observation points are probably due to complicated topography of their locations, which is not considered in the storm surge model. It is necessary to improve storm surge model in order to reproduce also such local complex phenomenon.

The absolute error in the estimation of storm surge is checked on the base of the results for the Suo Sea by $\Delta\eta^{Myers} = \left|\eta_{obs} - \eta^{Myers}\right|$ and $\Delta\eta^{mod}_{super} = \left|\eta_{obs} - \eta^{mod}_{super}\right|$. The mean absolute error $\overline{\Delta\eta^{Myers}} = 0.74\text{m}$, while this error reduced twice as $\overline{\Delta\eta^{mod}_{super}} = 0.37\text{m}$, when modified Myers pressure and super gradient wind are utilized.

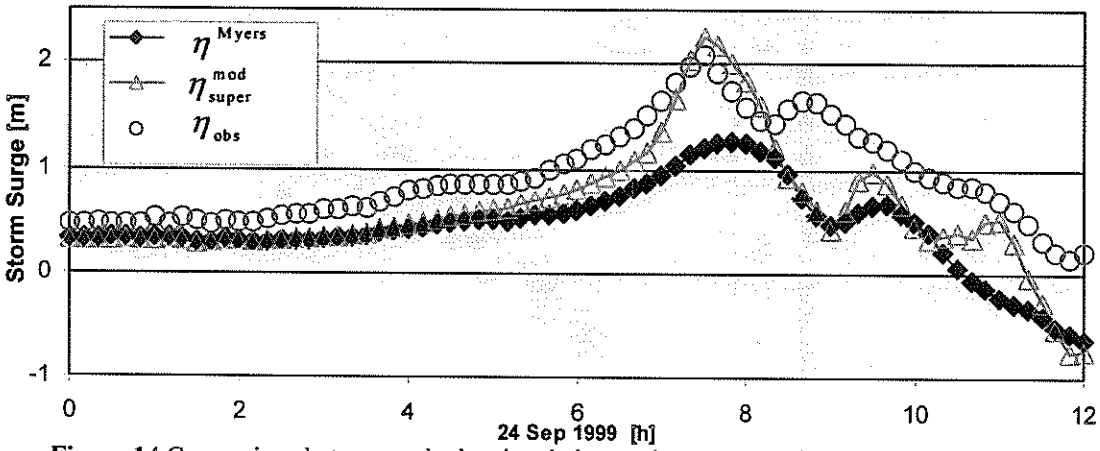


**Figure 14** Comparison between calculated and observed storm surge in the western Suo Sea

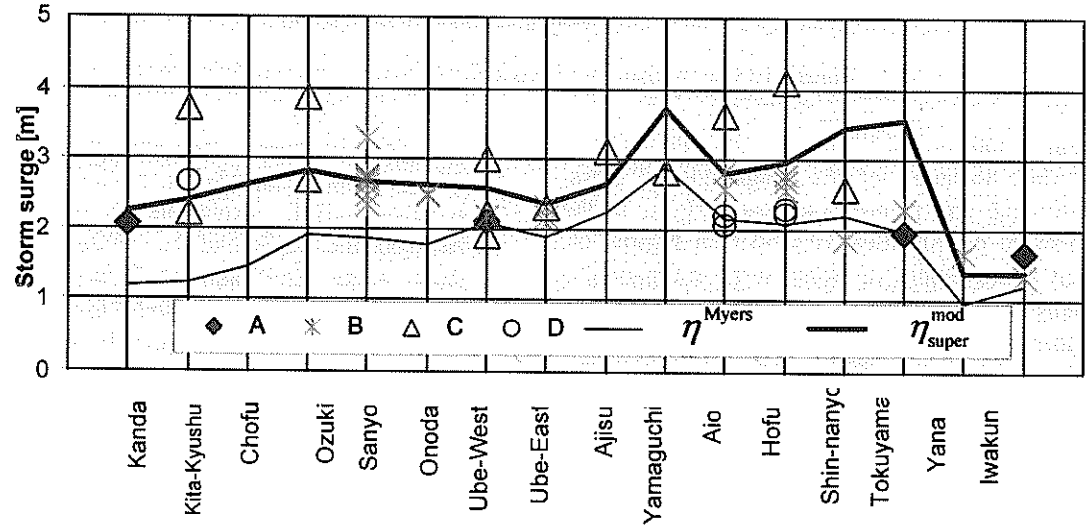


**Figure 15** Calculated and observed storm surge in different observation points in the Suo Sea

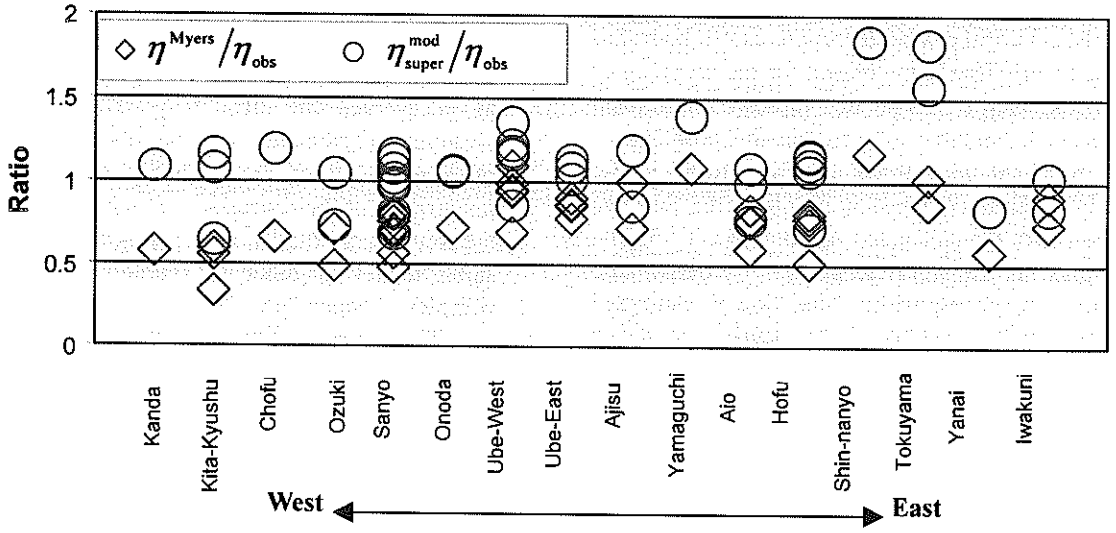


**Figure16** Ratio between calculated and observed storm surge in the Suo Sea

## 6. Conclusions

The pressure and wind distribution in a real typhoon is investigated on the base of data for four typhoons, attacked the Kyushu Island, Japan – T9918, T9119, T9117 and T9307.

The validity of Myers radial symmetric pressure distribution, widely utilized for the case of typhoons, is examined. In the front zone of the typhoon, the observed pressure is lower than the calculated by Myers formula. The obtained distortion from the radial symmetry of Myers distribution is parameterized as an analytical expression for the modified Myers pressure distribution is proposed. The modified Myers pressure distribution provided closer estimations to the observed ones in comparison with the Myers pressure formula.

The influence of the pressure distortion on the wind estimation is studied on the next step. The distortions in the pressure distribution lead to higher wind speed in the front zone of the typhoon. The combination of distorted pressure distribution, provided by the modified Myers pressure distribution and super gradient wind, increases the wind speed in the area, close to the radius of maximum wind of the typhoon. The comparison between the observed and calculated wind shows that the previous model underestimated the wind, while utilizing modified Myers pressure and considering vertical structure of typhoon through super-gradient wind leads to better agreement with observed winds. It is important to consider super gradient wind in the estimation of storm surge for the cases when the typhoon crosses an inner bay. The distortion of pressure distribution has to be taken into account during typhoon land approaching and landfall.

The response of the storm surge model to the corrected pressure and wind field is checked. The magnitude of storm surge is underestimated in the case of Myers pressure distribution used as input. Consideration of the pressure distortion by the modified Myers pressure distribution and super gradient wind in the typhoon leads to an improvement of storm surge estimation for the case of on shore directed wind.

More accurate diagnosis of the storm surge magnitude in coastal areas is achieved by the incorporation of the transformation of the typhoon structure due to land approaching and landfalling.

The results of this work contribute to the accurate hindcast of storm surge in the case of typhoons that crossed inner sea. More correct estimation of the extreme sea conditions for the area of an inner sea could be achieved by taking into consideration the distortion of atmospheric pressure and super gradient wind in the typhoon, obtained in this study. Additional studies are necessary in order to improve estimation of the storm surge in the coastal areas with complex topography, as well as to overcome the overestimation of the wind with offshore direction.

*(Received on February 14, 2002)*

**Acknowledgements**

This study has been supported by the Program for Promoting Fundamental Transport Technology Research from the Corporation for Advanced Transport and Technology (CATT), Japan.

Authors would like to appreciate to Dr. Kazumasa Katoh, now supervisor of Port and Airport Research Institute, for the idea to investigate the pressure distribution in the real typhoon, from where this study started two years ago. The critical review and suggestions from Dr. Shigeo Takahashi, Director of Marine Environment and Engineering Department, PARI, are gratefully acknowledged by authors.

**References**

Fujii, T. and Y. Mitsuda (1986) : Synthesis of a Stochastic Typhoon Model and Simulation of Typhoon Winds, Annuals Disaster Prevention Research Institute, Kyoto University, No.29 B-1, pp. 229-239.

Gray, W. M. and D. J. Shea (1973) : The Hurricane's Inner Core Region. II Thermal Stability and Dynamic Characteristics, Journal of Atmospheric Sciences, Vol.30, pp.1565-1576.

Gonnert, G., S.K. Dube, T.S. Murty and W. Siefert (2001) : Global Storm Surge – Theory, Observations and Applications, Archive for Research and Technology on the North Sea and Baltic Sea, 623p.

Houston, S. H., W. A. Shaffer, M. D. Powell, J. Chen (1999) : Comparison of HRD and SLOSH Surface Wind Fields in Hurricanes: Implications for Storm Surge Modeling, Weather and Forecasting, Vol.14, 670-686.

Jelesnianski, C.P. (1965) : A Numerical Calculation of Storm Tides Induced by a Tropical Storm Impinging on a Continental Shelf, Monthly Weather Review, 93, pp.343-360.

Kawai, H., T. Hiraishi, H. Maruyama and Y. Tanaka (2000) : Field Investigation and Numerical Simulation of Storm Surge by Typhoon No.9918, Technical Note of Port and Harbour Research Institute, No.971, 43p.

Mitsuta, Y, T.Fujii and K. Kawahira (1980) : Comparison of the Wind in the Gradient-wind-balance with the Moving Pressure Field and the Observed Surface Wind –

Preparation for Development of Technique for Simulation of the Surface Wind during Passage of Standard Project Typhoon, Annuals Disaster Prevention Research Institute, Kyoto University, No.23 B-1, pp. 1-9.

Murty, T. S. (1984) : Storm surges: Meteorological Ocean Tides, Bulletin 212, Department of Fisheries and Oceans, Ottawa, 897p.

Myers, V. A. and W. Malkin (1961) : Some Properties of Hurricane Wind Fields as Deduced from Trajectories, National Hurricane Research Reports No.49, U.S. Weather Bureau, Washington, DC. pp. 1-45.

Okamura, H. (2001) : Meteorological Condition of a Typhoon TY9918 (BART), Umi to Sora – Sea and Sky, Vol. 76, No.4, pp. 165-172.

Pagenkopf, J.R. and B.R. Pearce (1975) : Evaluation of Techniques for Numerical Calculation on Storm Surges, Report No.199, Department of Civil Engineering, MIT, MA. 120p.

Powell, M.D. (1982) : The Transition of the Hurricane Frederic Boundary-Layer Wind Filed from the Open Gulf of Mexico to Landfall, Monthly Weather Review, Vol.110, pp. 1912-1932.

"Sea and sky" (2001) - " Storm surges due to a typhoon TY9918 (BART) and their mechanism", Journal of Marine and Meteorology Society, Japan, Vol. 76, No.4, pp. 163-230.

Shea, D. J. and W. M. Gray (1973) : The Hurricane Inner Core region. I. Symmetric and Asymmetric Structure, Journal of Atmospheric Sciences, Vol.30, pp.1544-1564

Takayama, T. (2001) : Recent Disaster due to Storm Surges and Effective and Probable Measures against It, Proceedings of International Workshop on Advanced Design of Maritime Structures in 21st Century, PHRI, Japan, pp.162-171.

**List of Symbols**

| | | |
|---|---|---|
| $a^2$ | : | functional of differences |
| $C_j$ | : | center of the typhoon |
| $\vec{C}$ | : | speed of typhoon movement |
| $C_1(x)$ | : | coefficient of super gradient wind |
| $\partial/\partial$ | : | partial derivative |
| $d/d$ | : | full derivative |
| $f$ | : | Coriolis parameter |
| $i$ | : | index of observation points |
| $j$ | : | observation term |
| $k$ | : | drag coefficient |
| $N_{Front}$ | : | total number of points in Front zone |
| $O_i$ | : | observation point $i$ |
| $p_0$ | : | minimum typhoon central pressure |
| $p_n$ | : | ambient pressure at infinity |
| $p_i^{obs}$ | : | observed pressure at point $i$ |
| $p_i^{Myers}$ | : | Myers pressure at point $i$ |
| $r$ | : | radial distance from the center |
| $r_0$ | : | radius of maximum wind |
| $r_i$ | : | distance between $C_j$ and $O_i$ |
| $\{\bar{r}_0, r_{01}, r_{02}, \alpha_1, \alpha_2\}$ | : | parameters of modified Myers pressure distribution |
| $U_{Gi}$ | : | gradient wind |
| $V_c$ | : | cyclostrophic wind |
| $V_g$ | : | geostrophic wind |
| $\vec{V}^{Myers}$ | : | wind, calculated by Myers pressure distribution without super gradient wind |
| $\vec{V}^{Myers}_{super}$ | : | wind, calculated by Myers pressure distribution with super gradient wind. |
| $\vec{V}^{mod}_{super}$ | : | wind, estimated by the modified Myers pressure distribution with super gradient wind |
| $x = r/r_0$ | : | normalized distance by $r_0$ |
| $\alpha$ | : | inflow angle |
| $\gamma$ | : | parameter |
| $\vec{\gamma}_c$ | : | centrifugal acceleration |
| $\Delta p_i$ | : | difference between $p_i^{obs}$ and $p_i^{Myers}$ |
| $\Delta p^{Front}$ | : | mean value of $\Delta p_i$ in Front zone |
| $\Delta\eta^{Myers}$ | : | absolute error in estimation of $\eta^{Myers}$ |
| $\Delta\eta^{mod}_{super}$ | : | absolute error in estimation of $\eta^{mod}_{super}$ |
| $\overline{\Delta\eta^{Myers}}$ | : | mean value of absolute errors $\Delta\eta^{Myers}$ |
| $\overline{\Delta\eta^{mod}_{super}}$ | : | mean value of absolute errors $\Delta\eta^{mod}_{super}$ |
| $\varphi$ | : | latitude |
| $\tau$ | : | wind stress |
| $\rho_a$ | : | air density |
| $\eta_{obs}$ | : | observed storm surge |
| $\eta^{Myers}$ | : | storm surge, calculated by Myers pressure distribution without super gradient wind |
| $\eta^{mod}_{super}$ | : | storm surge, estimated by the modified Myers pressure distribution with super gradient wind |
| $\theta$ | : | angle between direction of typhoon movement and $O_i$ |
| $\vec{v}$ | : | wind velocity |
| $v_\theta$ | : | tangential component of $\vec{v}$ |
| $\vec{\omega}$ | : | angular velocity of the earth rotation |
| $\vec{\omega}\times\vec{v}$ | : | vector product of $\vec{\omega}$ and $\vec{v}$ |
| $\nabla p$ | : | pressure gradient |